Research Reports :

Reconstructions and Analyses of Neuronal Morphology Based on Metadata

Xing Yicai

Introduction

The study of neuronal morphology can be traced back to 30 years ago. Its importance has been widely recognized since the birth of neuroscience. Here they expound the role of axons and dendrites in synaptic integration, signal transmission, network connection and nervous system function, and requires quantitative analysis of digital three-dimensional reconstruction of neural morphology by circuit dynamics. The calculation method is necessary to quantify the complex relationship between neuron morphology (structure) and physiology. The three-dimensional digital reconstruction of axon and dendritic branches is indispensable to explore neural function.[1]

Neural morphology only represents neural morphology itself, but digital reconstruction will reveal more. Optical microscope can achieve the best balance between resolution and field of view, which is still the best choice for research[2]. The preprocessing steps of digital reconstruction are the same as those of pen and paper tracing: histological tissue preparation, staining and labeling, and imaging [3]. The staining method I plan to use to collect the data is rapid Golgi staining, and the kit I use is FD Rapid GolgiStain[TM] kit by biolead company of Beijing.

Morphological data belongs to image data, and the amount of information obtained through the subjective judgment of the naked eye is very limited. However, once the digital reconstruction is carried out, the morphological data can be reused in auxiliary applications outside the scope of the original project, including computational simulation, comparative analysis and large-scale data mining across laboratories or technologies. Only by quantifying the data with some unified indicators can it be easier to obtain more perfect raw data for big data analysis.

In this era when research is highly complex, many opensource data need to be published and researchers work together, a mature database in a field is very important. In just a few years, 866 laboratories around the world have contributed more than 100 thousands of neurons from over 50 different species and over 50 brain regions (chart 1, 2) for the open archive of neuronal reconstruction **NeuroMorpho.Org**. It will be the main database for my research.[4]

Scheduled research methods

Here, I will briefly introduce my experimental plan, and I will also introduce the reference materials of each part in detail later. (figure 1)

First, there are many opensource neuro-morphological data. Its structure probably includes 3D micrographs, morphological reconstruction manually drawn by researchers and digital data

containing various morphological indexes. After I get these data, I will first establish a database, which will be large enough for future study and work.

Figure 1. Schematic diagram of expected experiment flow

Then I will use the current mainstream image feature extraction algorithm to identify each component of neurons, and develop a set of algorithm that can automatically assist researchers to obtain the data required by the research literature, and finally output the results in a simple step. Finally, I will try with the results of my own laboratory to verify the feasibility of my algorithm.

Meta Data

Just as Zuckerberg's meta universe is the universe in the universe, secondary neuron digital data can also be called metadata.

NeuroMorpho.Org is open and free and can be accessed through any modern web browser, whether explorer, Firefox or Safari, and any operating system, including windows, MAC and Linux, without login / registration. The whole neuron morphology database can be browsed by cell type, brain region and animal species. The navigation of web pages is very simple and clear, and the database is also very large.

A separate neuron page, including download links of original and processed data files, information logs, images and dynamic display options, as well as indicators of experiments, literature and various morphological measurements.

Species (91)	#cells
mouse	64959
rat	45038
drosophila melanogaster	33498
human	8788
zebrafish	5484
monkey	3064
chimpanzee	1052
Xenopus laevis	743
Semipalmated sandpiper	634
C. elegans	600
Semipalmated plover	501
Clam worm	416
Baboon	401
Ruddy turnstone	392
giraffe	384
capuchin monkey	299
leopard	254
cheetah	233
Hamster	227
domestic pig	212
rabbit	203
sheep	203
Lion	189
elephant	174
clouded leopard	154
zebra finch	153
cat	151
ferret	149
guinea pig	149
humpback whale	143
cricket	127
Steller's Sculpin	123
goldfish	117
Tiger	105
turtle	92
Bonobo	83
African wild dog	82
agouti	80
Calango lizard	80
pouched lamprey	75
chicken	71
manatee	70
Zebra	70

minke whale	70
Rana esculenta	62
Crab	61
salamander	60
Blue wildebeest	58
blowfly	56
Toadfish	54
bottlenose dolphin	53
Apis mellifera	39
Domestic dog	37
Greater kudu	36
dragonfly	30
Caracal	29
Wallaby	27
Lemur	24
Mongoose	24
Aplysia	23
proechimys	17
Silkmoth	15
Scinax granulatus	15
bat	15
Rhinella arenarum	13
potto	12
locust	11
moth	11
Axolotl	10
Blind mole-rat	10
Xenopus tropicalis	10
red panda	9
porpoise	8
Treeshrew	7
hippopotamus	7
Western tarsier	6
Sea lamprey	6
Ranitomeya imitator	6
Orangutan	5
opossum	5
sloth	5
Not reported	5
giant anteater	4
Praying mantis (Hierodula membranacea)	3
spiny lobster	3
grasshopper	3
Gorilla	3

Crisia eburnea	1
drosophila sechellia	1
Praying mantis (Rhombodera megaera)	1
Mormyrid fish	1

Chart 1. Cell types included in metadata

Brain Regions (68)	#cells
neocortex	56324
hippocampus	29273
protocerebrum	9489
optic lobe	7800
retina	6339
peripheral nervous system	6238
basal ganglia	5946
main olfactory bulb	5943
amygdala	3634
spinal cord	3178
entorhinal cortex	2651
hypothalamus	2420
antennal lobe	2376
cerebellum	2296
ventrolateral neuropils	2166
cortex	2098
brainstem	1915
Not reported	1642
mesencephalon	1622
Central nervous system	1598
Right Mushroom Body	1581
lateral horn	1568
Right Adult Central Complex	1378
Left Adult Central Complex	1317
thalamus	1264
myelencephalon	1106
forebrain	924
ventral thalamus	704
somatic nervous system	580
endocrine system	525
Cochlea	511
subesophageal zone-(SEZ)	476
subesophageal ganglion	475
ventral striatum	459
Left Mushroom Body	451
subiculum	335
anterior olfactory nucleus	326
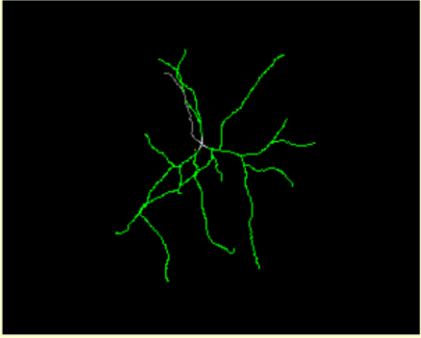
adult subesophageal zone	277
ganglion	242
pallium	222
pons	191
basal forebrain	162
corpus callosum	152
olfactory cortex	141
peptidergic circuit	106
antenna	96
olfactory pit	93
eye circuit	77
subpallium	65
retinorecipient mesencephalon and diencephalon	50
ventral nerve cord	37
stomatogastric ganglion	36
Central complex	33
abdominal ganglion	23
pharyngeal nervous system	20
accessory lobe	11
lateral line organ	6
accessory olfactory bulb	5
fornix	4
lateral complex	3
Pro-subiculum	3
meninges	2
parasubiculum	2
Subventricular zone	2
electrosensory lobe	1
nuchal organs	1
left	1
cerebral ganglion	1

Chart 2. Brian regions included in metadata

Here we find a simple data as an example.
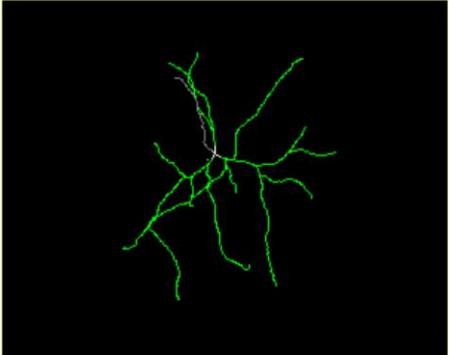
Figure 2. Brief introduction page of data

Open the web page of the database. When we click the metadata in the search, we can see the thumbnail page in Figure 2. We can see that this is a mouse cell, which contains three components: axon, dendrite and cell body. It is a nerve cell with complete structure. Click on the name of the cell and we get detailed information.

Figure 3. detailed information. Here, we can get files with fixed format.
http://neuromorpho.org/neuron_info.jsp?neuron_name=L7b2AKE

Evidence for elevated nicotine-induced structural plasticity in nucleus accumbens of adolescent rats

C.G. McDonald*,1, A.K. Eppolito1, J.M. Brielmaier, L.N. Smith, H.C. Bergstrom, M.R. Lawhead, R.F. Smith

Department of Psychology, George Mason University, MS 3F5, Fairfax, VA 22030, USA

Figure 4. the source of the data[5]

In this article, scientists administered nicotine tartrate to male rats during puberty (p29-43) or adulthood (p80-94). Five weeks after nicotine administration, the researchers stained the brain with Golgi and digitally reconstructed medium spinous neurons from the shell of the nucleus accumbens (NAC) for morphometric analysis.
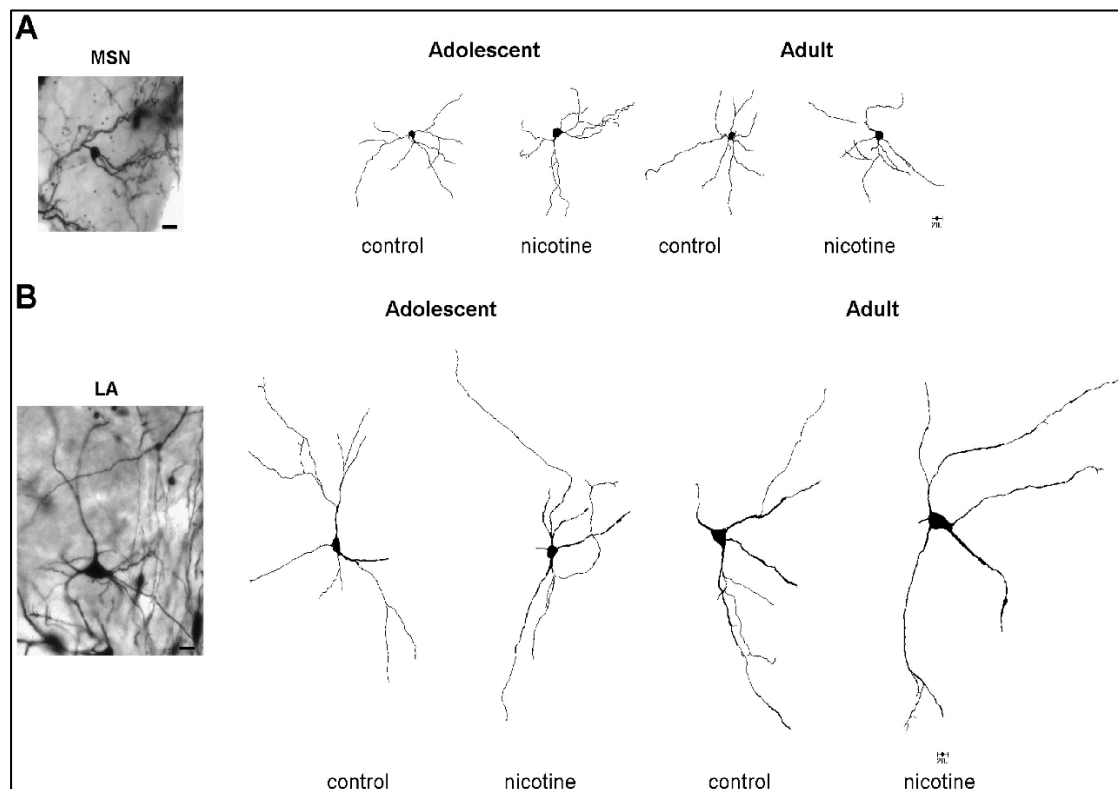

Figure 5. part of the data from the article. (scale: 20 μm)

From the above figure, we can see that after the author treated the brain tissue with Golgi staining, the representative micrographs and digital reconstruction of medium spinous neurons (a) and large spinous neurons (b) were recorded by microimaging. Because this article is a morphological article, the author also recorded detailed morphological data, specifically including:

Soma Surface :   577.63 μm^2
Number of Stems :   4
Number of Bifurcations :   10

Number of Branches :   24

Overall Width :   186.4 μm

Overall Height :   248.55 μm

Overall Depth :   57.41 μm

Average Diameter :   0.7 μm

Total Length :   1533.28 μm

Total Surface :   3552.16 μm²

Total Volume :   955.98 μm³

Max Euclidean Distance :   163.79 μm

Max Path Distance :   221.92 μm

Max Branch Order :   4

Average Contraction :   0.9

Total Fragmentation :   1202

Partition Asymmetry :   0.36

Average Rall's Ratio :   0.91

Average Bifurcation Angle Local :   80.34°

Average Bifurcation Angle Remote :   75.03°

Fractal Dimension :   1.03

The simplest way to improve the invariance of neural network is to expand our data set, which is the so-called data augmentation. In this way, there are more than 100000 detailed data obtained by Golgi staining, which is enough for us to do algorithm training.

Unified indicators

In the study of neuron morphology, a single morphological parameter does not have substantive research reference value, and a number of basic parameters and their correlation need to be studied. These basic parameters include the number of fibers or axons, perimeter and nerve cell body area. Based on the basic parameters obtained above, other parameters with high research value can be calculated: the ratio of myelin sheath thickness to axon diameter; Ratio of axon diameter to fiber diameter.

There are several methods to describe dendritic tree by fractal measurement, including mass radius method, box counting method and expansion method. In 1986, the cumulative crossover method for fractal analysis of neuron dendritic tree was proposed. This method is based on the method described by sholl[6].

This method uses concentric circles in two dimensions or spherical shells centered on cell bodies in three dimensions. If a neuron corresponds to a 3D fractal. The relationship between the total length N of all branches in the shell with radius R should follow the power law N (R) ~ R^{D}[7].

Therefore, at a given position R, the number of branches n (R) from the soma body is approximately determined by:

$$n(R) \sim \frac{dN(R)}{dR} \sim R^{D-1}$$

By calculating the cumulative number of intersections n(R) between branches and shells with increased radius r, the slope of the logarithmic relationship between the cumulative intersection number and radius is calculated by linear regression. The fractal dimension is obtained. Fractal analysis is widely used in the field of neuroscience. Many authors use **fractal dimension** to discuss the classification system of neurons, and prove that fractal dimension can classify different types of neurons from superior colliculus, retina, spinal cord and cortex.[8]

Fractal theory is widely used in image and signal analysis. Although fractal dimension can be used as image object descriptor, multi-scale methods (such as multi-scale fractal dimension (MFD)) will increase the amount of information extracted from objects.

Since MFD is independent of size related parameters such as surface area and volume, it is particularly suitable for studying ontogeny and phylogenetic changes at the level of some neuron types. For example, until recently, multiscale fractal analysis was used to quantitatively characterize the phenotype of pyramidal neurons in synras transgenic mice. Compared with wild-type pyramidal neurons, this suggests that enhancer activity in transgenic mice may lead to greater morphological changes in cell phenotype[9].

These mathematical methods are favorable for further data processing, so they are very suitable to be written into the program as a tool.

Algorithms Used in the Past

The reconstruction of neural morphology requires the development of neuron tracking methods, that is, the method of automatically tracking neural processes. In recent years, it has been a great challenge in computational neurobiology. At present, many scientists have developed some algorithms one after another.

3D skeletonization

Skeleton extraction, also known as binary image thinning. This algorithm can refine a connected region into a pixel width for feature extraction and target topology representation.

The morphology sub module provides two functions for skeleton extraction:
skeletonize () function and media function_axis() function. Format is skimage morphology. skeletonize(image), both input and output are binary images.[10]

Yuan proposed a method for tracking dendrites and dendritic spines based on 3D skeletonization. Different from the previous voxel based skeletonization methods, this method recursively follows the neuron topology, uses a set of 4 x N2 direction kernel and is guided by a generalized three-dimensional cylinder model. Firstly, the commercial deconvolution software package is used to preprocess the image, and then the anisotropic diffusion algorithm is used to smooth the image to retain the useful edges. In order to extract the skeleton from the gray preprocessed image, this method detects the critical point of the gradient vector field, that is, saddle point or attraction point. The skeleton starts from a saddle point and moves along its positive eigenvector in a voxel step until it meets a point of attraction.

Repeat this process until all saddle points are used as starting seed points. Neurite traces were obtained in three steps. Firstly, all skeleton points are regarded as vertices; Secondly, the strength weighted minimum spanning tree (iw-mst) is calculated. Thirdly, the iw-mst is refined using the minimum descriptor principle, because it may contain some errors. The method was tested on M1 and M2 mammalian data sets.[11]

Open-curve snake model
Wang proposed a three-dimensional neuron tracking algorithm based on open curve active contour, also known as open curve snake model.

After preprocessing, they calculated the gradient vector flow as the deformation force of the open curve snake. Then, the resulting image is binarized by using frangi's veselness filter and graph cutting segmentation algorithm. Next, the method selected by the user is applied to the binary image to define the seed set. Then the seeds are sorted according to the priority criteria, and the open snake tracking model is initialized at the first seed point.
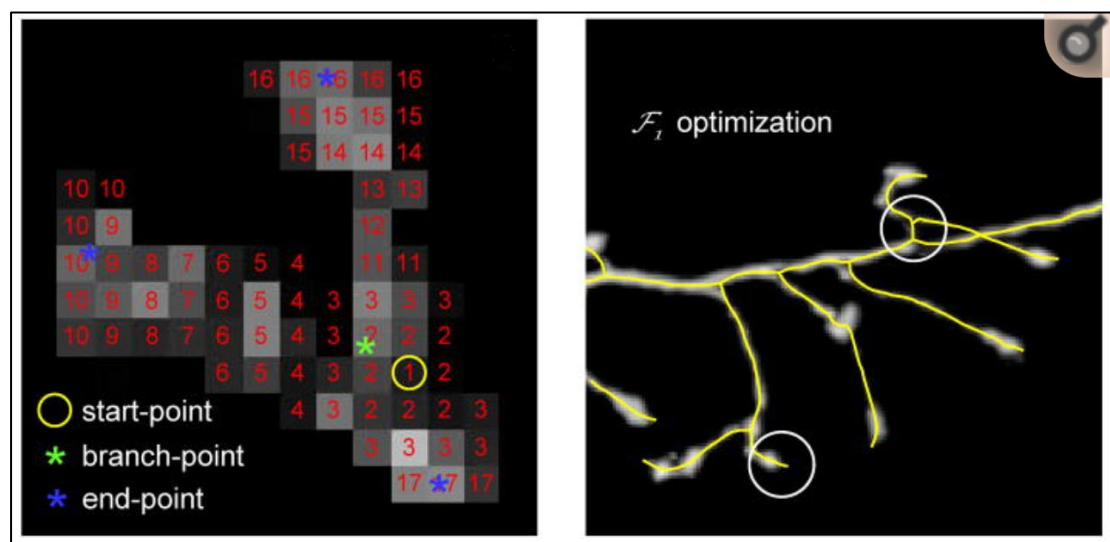

Figure 6. open-curve snake model

Voxel coding and tracking optimization. One. The maximum intensity projection of a small part of a dendritic tree. The 3D wave of continuous digital labels starts at any voxel (yellow circle) in the image. In each subsequent step of the algorithm, the new wavefront is determined as a group of unmarked image voxels near the current front voxel.

In each iteration, the snake grows, and the snake's energy function is minimized. The process stops when the maximum number of iterations is reached, or when the snake touches the image boundary, or when the length of the snake remains unchanged within the predefined number of iterations. Next, when a set of rules is rejected, it will not be verified. If the snake is not rejected, the seed list is updated and any seeds closer to the new trace than the user-defined threshold are deleted. This process starts from the next seed and continues until there are no seeds left. This method detects a branch point as the collision point of two snakes. The algorithm is tested on synthetic data sets and OP, CCF and NMF data sets of DIADEM challenge. Different methods are used to evaluate performance: the author uses DM3 metric on synthetic dataset, DIADEM metric

on CCF dataset and LM2 metric on NMF dataset.[12]

Fitness function, Φ 1. It is composed of the integrated strength along the trace (the average strength along the trace multiplied by the trace length) and the elastic energy of the trace:

$$F_1\left(\left\{\vec{r}_k\right\}\right) =$$

$$\sum_k \left(\frac{1}{\lambda} \sum_i I\left(\vec{R}_i\right) s^3 \frac{e^{-\left\|\vec{r}_k - \vec{R}_i\right\|^2/2\sigma^2}}{(2\pi)^{3/2}\sigma^3} - \frac{a_1\lambda}{2} \right.$$

$$\left. \sum_l \left\|\vec{r}_k - \vec{r}_{kl}\right\|^2 \right).$$

FM and hierarchical pruning

Xiao and Peng from Chinese Academy of Sciences proposed an automatic neuron tracking algorithm based on hierarchical pruning of gray weighted image distance tree. This is a new version of the full path pruning algorithm, which aims to generate more accurate reconstruction in a shorter time. This method is also known as full path trim 2.0. Threshold is the first step in providing background and foreground. Then, the grayscale weighted distance transform is calculated for all foreground pixels, so their intensity will be replaced by the sum of pixel intensities on the shortest path from the considered pixel to the background. The initial neurite reconstruction is given by the shortest path from a single point to another foreground pixel, which is obtained by Dijkstra algorithm. Because the result is the over reconstruction of neurons, the initial tree is removed to the level of a single neuron segment. Each neuron segment connects two branch points and is sorted in hierarchical order: the first and most important segment is the longest path from the source node to the farthest leaf node. This segment will be deleted from the initial tree and the longest path search will be repeated until there are no points left in the initial tree. Then, the pruning process is performed to discard the less important segments that overlap the more important segments. The method is tested on diadem OP dataset and Nm2 and Nm3 dataset. The distance metric DM3 is used to evaluate the performance of the algorithm.

G-Cut

Li Rui of Xiamen University reported a computing method called g-cut in 2019 to solve the challenge of reconstructing dense interleaved neurons. G-cut can automatically and robustly segment a single neuron from the neuron cluster according to the combination information of morphological features and the relationship between mixed neural processes. The estimation of the correlation between a single neurite and the body is based on the morphological information obtained from the existing large neuron morphological data set. Using synthetic data sets from tissue blocks and real image stacks, we demonstrate that g-cut achieves higher single neuron segmentation accuracy in neuronal clusters with various marker densities and morphological patterns than other most advanced algorithms. In short, g-cut is a powerful and powerful informatics tool, which is widely used in the morphological reconstruction of a large number of neurons, thus accelerating the cataloguing process of brain neuron cell types.

Preset possible algorithm

I personally hope to try more advanced algorithms and apply image recognition technology to neurobiology. At present, most Golgi staining neuron reconstruction algorithms are based on gray recognition.

Gray scale uses black tone to represent the object, that is, black is used as the reference color, and black with different saturation is used to display the image. Each grayscale object has a luminance value from 0% (white) to 100% (black). Images generated using black-and-white or grayscale scanners are usually displayed in grayscale. The value of gray level can be obtained by gamma correction.

$$Gray = \sqrt[2.2]{\frac{R^{2.2} + (1.5G)^{2.2} + (0.6B)^{2.2}}{1 + 1.5^{2.2} + 0.6^{2.2}}}$$

The key factor for us to recognize objects is gradient (many feature extraction, hog, LBP, sift and so on are essentially gradient statistical information). Gradient means edge, which is the most essential part, and the calculation of gradient is most commonly used as gray image. Grayscale is actually to reduce the dimension of the image, which can greatly reduce the amount of calculation. The demand for the computing power and recognition speed of the equipment is a key point for you to choose. Sometimes the grayscale image is still too large, and it is also possible to use binary image. In other words, the gray image is a two-dimensional matrix, and each pixel is a data.
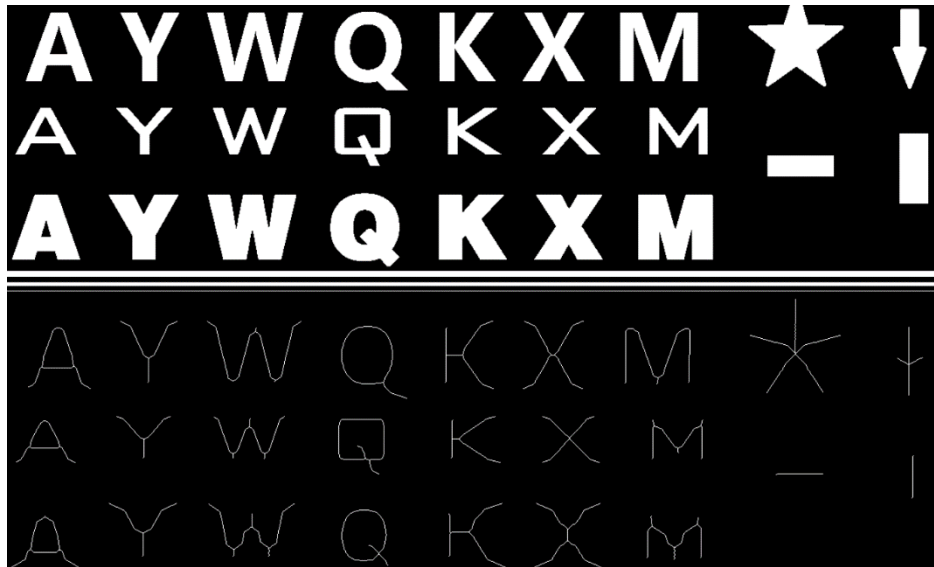

Figure 10. binary image thinning algorithm

So far, I think the most reliable method is the binary image thinning algorithm based on deep learning. There are many kinds of image thinning algorithms, which can be divided into iterative method and non-iterative method. Iterative method is divided into serial algorithm and parallel algorithm according to whether it processes pixels in parallel. In the parallel algorithm, the deletion of pixels has nothing to do with the order of pixel values in the image, but only depends on the result of the last iteration. In the serial algorithm, whether to delete pixels is not only related to the result of the last iteration, but also related to the distribution of current pixel values. At present, the typical algorithms are ZS image thinning algorithm, LW thinning algorithm and EPTA algorithm. ZS algorithm is a parallel thinning algorithm based on 8-neighborhood. It is the most

widely used algorithm at present. Its outstanding advantages are high algorithm efficiency, few iterations of the algorithm, and the shape consistent with the original image can be maintained for elements such as straight lines after thinning. LW algorithm improves the problem that ZS algorithm will lose local information, but it produces the problem of redundant bifurcation. EPTA is an enhancement of ZS algorithm and LW algorithm, which improves some problems of ZS and LW algorithm, but it has the problem of incomplete thinning of some images.

To solve this problem, we must have a very systematic knowledge of image recognition. In the process of finding prominence, we should rely heavily on binary image thinning algorithm. When looking for soma body, I think we should also use some clustering algorithms in addition to binarization.

In the past, I have seen a nuclear detection algorithm based on gray-scale morphological reconstruction, which obtains the initial candidate nuclear centroid based on gray-scale morphological reconstruction, refines the atomic nuclear centroid by searching the nuclear boundary from the centroid in the morphological gradient image, and removes the redundant centroid according to the rules related to distance, Finally, fuzzy C-means (FCM) or support vector machine (SVM) are used to identify the true nuclear centroid from other atomic nuclear centroids. This method is perhaps suitable for detecting soma body.[13]

In recent years, convolutional neural network (CNN) has achieved unprecedented success in the field of computer vision. At present, many traditional computer vision algorithms have been replaced by deep learning. Due to its huge commercial value, deep learning and convolutional neural network have become the focus of research, and a large number of excellent work continue to emerge. The subject at hand is also mainly image recognition. [14]

The methods used to identify dendrites and axons from microscopic images must not be much different from those used to identify cats and dogs. Image recognition is the core and basic problem in the field of computer vision. Other tasks such as target detection, image segmentation, image generation, video understanding and so on are highly dependent on the ability of feature expression in image recognition. The latest progress of convolutional neural network in image recognition can directly affect the performance of all computer vision tasks based on deep learning, so it is particularly important to deeply understand this progress.

A simple convolutional neural network is composed of various layers arranged in order. Each layer in the network uses a differentiable function to transfer data from one layer to the next. Convolutional neural network is mainly composed of three types of layers: convolution layer, pooling layer and full connection layer. By superimposing these layers, a complete convolutional neural network can be constructed.[15]

Convolution layer can be said to be one of the most important steps in convolution neural architecture, which involves the quality of feature expression. At the same time, it also accounts for more than 95% of the computation of our whole network. Convolution is a linear and translation invariant operation.

The nonlinear activation unit is inspired by the neuron model of human brain. In the neuron model, dendrites transmit signals to the cell body, and the signals are combined and added in the cell body. If the final sum is higher than a certain threshold, the neuron will activate and output a peak signal to its axon to the next neuron.

The main purpose of introducing nonlinear activation function is to increase the nonlinearity of neural network. Because if there is no nonlinear activation function, the output of each layer is a linear function of the input of the upper layer. Therefore, no matter how many layers the neural network has, the output is a linear function, which is the original perceptron model. This linearity is not conducive to giving full play to the advantages of the neural network.

The common non-linear activation units are ReLu and LReLu, Logistic and Igmoid, and sigmoid gradually exits the stage of history due to the disappearance of the entire network gradient due to its saturation characteristics.
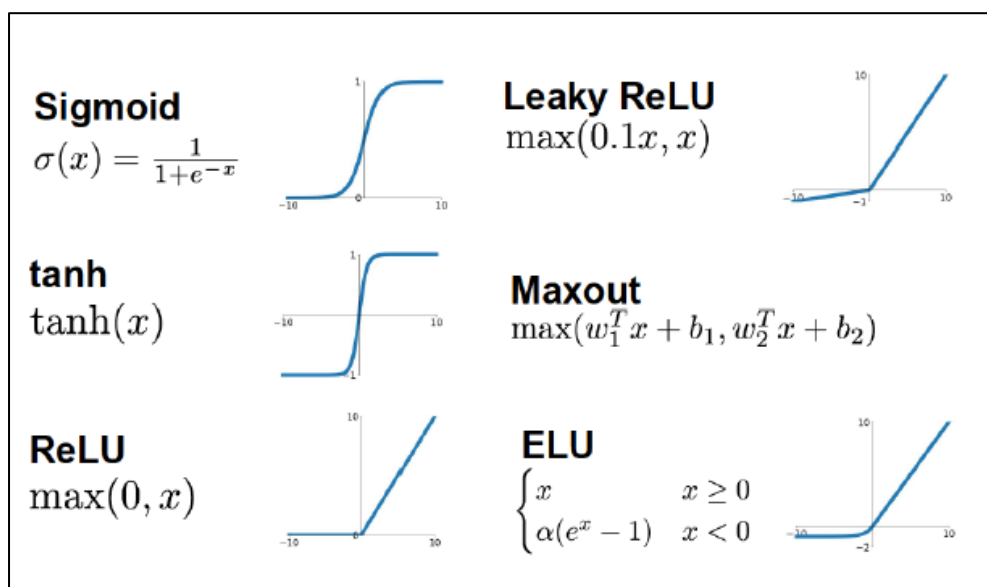

Figure 11. common non-linear activation units

Generally, a pooled layer is periodically inserted between consecutive convolution layers. Its function is to gradually reduce the spatial size of the data volume, which reduces the number of parameters in the network, reduces computational resource consumption, and effectively controls over-fitting, as shown in Figure 5. The pooling layer usually uses MAX operations to operate independently on each slice of the input data volume, changing its spatial size. The most common form is to use a filter of size 2x2 to downsample each depth slice at a step of 2, losing 75% of the activation information. Each MAX operation takes the maximum of four numbers. During pooling, the number of channels in the data volume remains constant.

The so-called full-link layer is the traditional neural network, where each neuron unit is densely connected to all the neurons in the upper layer. Nowadays, due to its large number of parameters that are easy to fit and do not conform to the principle of human local perception of images, full-join layers generally do not participate in image feature extraction (replaced by convolution layers) and are only used for the final linear classification, which is equivalent to a linear

combination on the extracted high-level feature vectors and outputs the final prediction results.[16]

The latest convolution neural network solves to some extent the problem of feature expression in the field of computer vision, which has made a lot of achievements and was very hot in the past few years.

Conclusion

The end result should be a very complex algorithm, but no matter what algorithm I use, I want the neurobiology experiments to be more automated and more convenient, and I want my settings to provide a convenient tool for experiments of other.

References

1. Halavi, Maryam, Kelly Andrew Hamilton, Ruchi Parekh and Giorgio A. Ascoli. "Digital Reconstructions of Neuronal Morphology: Three Decades of Research Trends." Frontiers in Neuroscience 6 (2012).
2. Lu, J. Neuronal Tracing for Connectomic Studies. *Neuroinform* **9,** 159–166 (2011).
3. Meijering, E. Neuron tracing in perspective. Cytometry A 77, 693–704. (2010).
4. Halavi, M., Polavaram, S., Donohue, D. E., Hamilton, G., Hoyt, J., Smith, K. P., and Ascoli, G. A. NeuroMorpho.Org implementation of digital neuroscience: dense coverage and integration with the NIF. Neuroinformatics 6, 241–252. (2008).
5. McDonald, C. G., Eppolito, A. K., Brielmaier, J. M., Smith, L. N., Bergstrom, H. C., Lawhead, M. R., & Smith, R. F.. Evidence for elevated nicotine-induced structural plasticity in nucleus accumbens of adolescent rats. Brain research, 1151, 211–218. (2007)
6. D. A. Sholl,"Dendritic organization in the neurons of thevisual cortices of the cat, J. Anat., 87,387-406(1953).
7. A. Schierwagen,Scale-invariant diffusive growth: Adissipative principle relating neuronal form to function, inOrganizational Constraints on the Dynamics of evolutionJ. Maynard-smith and g. Vida(eds) Manchester UniPress, Manchester(1990), pp. 167-189.
8. P Meakin,A new model for biological pattern formationJ. Theor:Biol., 118,101-113(1986)
9. A. Schierwagen, L. F. Costa, A. Alpar, et al., "Neuromorphological phenotyping in transgenic mice: a multiscale fractal analysis," in: Mathematical Modeling of Biological Systems, Vol. II, A. Deutsch, R. Bravo de la Parra, R. de Boer, et al., (eds.), Birkhäuser, Boston, 2007, pp. 191-199.
10. K. Palágyi, A. Kuba:A parallel 3D 12-subiteration thinning algorithm,Graphical Models and Image Processing 61, 1999, 199-221.
11. Al-Kofahi, K., Lasek, S., Szarowski, D.H., Pace, C.J., Nagy, G., Turner, J.N., Roysam, B., & et al. Rapid automated three-dimensional tracing of neurons from confocal image stacks. IEEE Transactions on Information Technology in Biomedicine, 6(2), 171–187. (2002).
12. Wang, Y., Narayanaswamy, A., Tsai, C.L., & Roysam, B. A broadly applicable 3-D neuron tracing method based on open-curve snake. Neuroinformatics, 9(2-3), 193–217. (2011).
13. Plissiti ME, Nikou C, Charchanti A. Automated detection of cell nuclei in pap smear images using morphological reconstruction and clustering. IEEE Trans. Inf. Technol. Biomed.15(2):233–241. (2001)
14. A. Krizhevsky, I. Sutskever, and G. E. Hinton. Imagenet classification with deep

convolutional neural networks. In Advances in neural information processing systems, pages 1097–1105, (2012).

15. C. Szegedy, W. Liu, Y. Jia, P. Sermanet, S. Reed, D. Anguelov, D. Erhan, V. Vanhoucke, and A. Rabinovich. Going deeper with convolutions. In Proceedings of the IEEE Conference on Computer Vision and Pattern Recognition, pages 1–9, (2015).

16. Heaton, J. Ian Goodfellow, Yoshua Bengio, and Aaron Courville: Deep learning. Genet Program Evolvable Mach 19, 305–307 (2018).